JJEES

JJEES (2023) 14 (1): 9-18
ISSN 1995-6681

Jordan Journal of Earth and Environmental Sciences

Geospatial Soil Suitability Assessment for Maize (Zea mays) Production in Derived Savanna of Agricultural Research and Training, OYO STATE, Nigeria

Anthony Tobore[1*], Bolarinwa Senjobi[1], Ganiyu Oyerinde[2], Samuel Bamidele[3]

[1]Department of Soil Science and Land Management, Federal University of Agriculture Abeokuta, Ogun State, Nigeria. P.M.B. 2240, Abeokuta, Ogun State, Nigeria.
[2]Department of Soil Science, Faculty of Agriculture, University of Abuja, Nigeria
[3]Department of Plant & Soil Sciences, University of Delaware, 531 S. College Avenue, Townsend Hall Rm. 152, Newark, DE 19716, USA

Received 21st September 2021; Accepted 19th May 2022

Abstract

The study focused on the geospatial assessment of the physicochemical properties of soils at the Institute of Agricultural Research and Training, Ilora, Oyo State, Nigeria. Using the random survey method, 100 surfaces (0 to 20 cm) samples were collected and subjected to standard soil laboratory analyses. The variability of soil nutrients was examined using descriptive statistics, while spatial investigation and interpolation were achieved using the Ordinary krigging (OK) method. Cross-validation accuracy with exponential and spherical models was used as a precision tool for the analyzed soil nutrients. Soil nutrient spatial trends were exponentially distributed across the area. Temporal predicted land surface temperature (LST), and soil-adjusted vegetation index (SAVI) were estimated through Landsat images of the years 2000 and 2020 using ArcGIS 10 software. The spectral variables – LST and SAVI were merged with soil nutrients to assess the maize suitability evaluation of the area. The LST and SAVI results revealed the qualitative differences in the studied area. The maize suitability showed that the studied soils ranged from moderately (85%), marginally (60%), and not suitable (< 40%). To increase the suitability of the soils for optimum maize production there is a need to enhance the limiting dominant factors such as undulating topography, rainfall, and erosion hazard. Hence, the study recommends the integration of geospatial techniques such as remote sensing covariate variables and exponential models as indispensable methods to assist farmers and policymakers in sustainable and precision agriculture.

Keywords: *Geospatial approaches: Maize suitability; Ordinary krigging; Soil nutrients: Derived savanna.*

1. Introduction

Variability assessment of the soil nutrients is considered a fundamental step required for sustainable precision farming (Ge et al., 2007). The major factor limiting food production in most developing countries can be traced to the inappropriate and abuse of soils (Ekeleme et al., 2014). For instance, in Nigeria, soil properties are faced with anthropogenic activities such as the illegal felling of trees, and abuse of pesticides and fertilizers, etc. (United Nations, 2017). Moreover, Adekiya and Agbede (2009) also stated that derived Savanna soils are prone to nutrient soil loss which led to crop failure, especially maize. Maize (Zea mays) is an agroecological staple crop cultivated worldwide (Liu et al., 2015). Nevertheless, attaining optimum yield of crop such as maize in ever-changing environments, require the need to assess the soil nutrients such as physical and chemical properties using geospatial approaches (Liu et al., 2015).

Moreover, Remote sensing techniques (RST) are becoming acceptable methods and decision-support techniques used for modeling and mapping the physical and chemical properties of soils especially when precision agriculture is desired (Carlson et al., 1994). Additionally, multi-criteria assessment using the Analytical hierarchy technique (AHT) has been used as a bottom-up approach to monitoring changes in soil properties (Marko et al., 2014). Besides, many researchers have utilized the Ordinary kriging (OK) method to interpolate and predict un-sampled points for site-specific studies (Zhang et al., 2010). For example, Martey et al., (2014) utilized Landsat imageries to map soil properties using spectral indices such as predicted land surface temperature (LST) and predicted soil-adjusted vegetation index (SAVI). The research concluded that LST and SAVI gave a better qualitative accuracy on soil nutrients.

Despite the widespread use of these geospatial approaches, studies on soil properties using multi-criteria evaluation coupled with remote sensing and geostatistical modeling are still lacking in implementation in Nigeria. Hence, the study seeks to integrate the AHT to evaluate spatial changes of soil nutrients at the Institute of Agricultural Research and Training (IAR&T), Ilora, Oyo State, Nigeria using LST, SAVI, and OK interpolation models such as exponential and spherical. More specifically, the study is targeted to map variability changes in soil nutrients for maize production using geospatial approaches. Therefore, the study objectives are:

1. To assess and interpolate the soil physical and chemical nutrients of the study area.
2. To produce a maize soil suitability map using PLST, PSAVI, and OK interpolation models.

* Corresponding author e-mail: toboreao@funaab.edu.ng

2. Methods

2.1 The study region

The study area lies at the transitionally derived savanna with mixed rolling topography in Nigeria within Northing $7^0$48’5 N and $7^0$49’4 N and Easting $3^0$49’0 E and $3^0$44’5 E (Fig. 1). The relative humidity mean within the study area falls between 60 % with 90 days cumulative rainfall (FDALR, 1990). The soils of the study area originated from basement complex parent material (USDA, 1999).

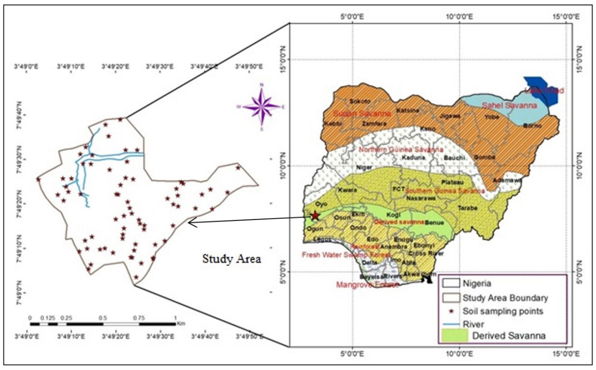

Figure 1. Agro-ecological (Nigeria) zones showing the soil sampling in the study area.

2.2 Assessment of soil properties using remote sensing variables

The dependent variables used in this study include existing roads, rivers, predicted soil-adjusted vegetation index (SAVI), and predicted land surface temperature (LST). The remote sensing variables – SAVI and LST were used to assess and monitor changes in soil properties through the acquired Landsat images of the years 2000 and 2020 (Gilabert et al., 2002). The Landsat images were obtained freely from the United States Geological Survey (USGS) repository website. The satellite images were downloaded using path 191 and row 055 and georeferenced with World Geographic System (WGS) 84 datum (Jiang et al., 2006; Jeevalakshmi, 2017). The images were downloaded during low cloud cover to avoid seasonal variation and mitigate disruption in data sets (Table 1).

Table 1. Spectral index used for the present study.

Landsat 7 ETM+	Landsat 8 OLI/TIR
B-3:Red (0.631 – 0.69um)	B-4: Red (0.636 – 0.673um)
B-4: Near-infrared (0.77 – 0.90um)	B-5: Near-infrared (0.77 – 0.90um)
B-6: Thermal (10.40 – 12.50 um)	B-10&11: Thermal infrared 1&2 (10.60 – 11.19um) & (11.50 – 12.51um)

B: denotes Bands, OLI: Operational land image

2.3 Predicted soil-adjusted vegetation index (SAVI)

To perform the SAVI, Dorigo et al., (2007) formula was used in ArcGIS 10 ESRI (Environmental software research Institute) in equation (1).

$$SAVI = \frac{(\mathrm{NIR} - \mathrm{RED})}{\mathrm{NIR} + \mathrm{RED} + \mathrm{L}}(1 + L) \quad (1)$$

Where NIR is the Near-infrared representation, RED is the visible red, and L is the constant or correction factor (Huete, 1988).

2.4 Predicted land surface temperature assessment

The Predicted land surface temperature (LST) variables were often used to monitor soil temperature changes and serve as an important spectral index that provides fundamental information for human survival (Cai et al., 2018). In this study, two steps were employed to assess the PLST. To perform the first step using Landsat 7, the spectral index of band 6 was used (Cai et al., 2018):

$$R\tau m^6 = \frac{V}{255(R_{\max} - R_{\mathrm{mln}})} + R_{\mathrm{min}} \quad (2)$$

The R_{TM6} denotes luminance of radiation; digital numbers of band 6 were used to represent the V. Rmaximum = 1.896: Rminimum = 1.896". Thereafter, equations (3) and (4) were used to convert the PLST (luminance radiation) into kelvin and degree Celsius.

$$T_k = \frac{K_1}{ln\left\{\frac{K_2}{\mathrm{RTM6}\ /b}\right\} + 1} \quad (3)$$

K_1 = 1260.56; K_2= 607.66. The K_1 and K_2 are constant and 1.239 (µm) spectral ranges were used to represent b.

$$T^0c = T_k - 273 \quad (4)$$

Thereafter, Vegetation proportion (VP) data derived from the year 2020 in equation (1) were used to support the estimation of the PLST for the year 2020. The PLST estimation was expressed in equation (5):

$$VP = \left(\frac{\mathrm{PSAVI} - \mathrm{PSAVI}_{\min}}{\mathrm{PSAVI}_{\max} - \mathrm{PSAVI}_{\min}}\right)^2 \quad (5)$$

The PSAVI $_{min}$ and $_{max}$ was derived from the minimum and maximum value of PSAVI. The PSAVI value ranges from -1 and 1. Equation (6) was used to assess the VP of the study area.

$$VP = \left(\frac{\mathrm{SAVI} + 1}{2}\right)^2 \quad (6)$$

The Landsat 8 Operational land images (OLI) were used to perform step 2. The digital numbers (DNs) of bands 10 and 11 were used to estimate the (spectral radiance, (LSE) Land surface emissivity, and (BT) Brightness temperature (Rasul et al., 2015). For the year 2020 PLST, the equations described by Jesus and Santana (2017) were used to assess the LSE, BT, and of the study area.

$$L\lambda = 0.03342 * \text{spectral band10} + 0.1 \text{ and spectral band11} + 0.1 \quad (7)$$

$$LSE = 0.004 * PV + 0.986 \quad (8)$$

$$BT = \frac{K2}{ln\left\{\frac{K1}{L\lambda}\right\} + 1} - 273.15 \quad (9)$$

BT is measured in Celsius; K1 and K2 are the thermal calibrations constant and both are measured in Kelvin.

$$PLST = \frac{BT}{1(\frac{\lambda BT}{PV} * \ln LSE)} \quad (10)$$

2.5 Soil Analyses and Spatial mapping

Random and reconnaissance sampling method was employed using FAO (2007) soil survey manual. With the aid of a soil auger, 100 samples were collected at 0 to 20 cm soil depths and their coordinate points were tied to each sampling point and documented using a global positioning system (GPS) device. Afterward, the representative soil samples were further subjected to 2 mm diameter sieving and air-drying before being taken to routine soil laboratory analysis. Particle size distribution was examined using the hydrometer method (Bouyoucos, 1962). Soil pH was determined using a pH glass meter electrode in 1:2

suspensions of water (McLean et al., 1982). Organic carbon (OC) was examined by Walkley and Black, (1939) using the acid chromic oxidation method. Total nitrogen (TN) was examined using the Macro Kjeldahl method (Bremner and Mulvaney, 1982). Available phosphorus (P) was determined by the Bray-1 method (Nelson and Sommers, 1996). The potassium (K) was examined by a flame photometer (Kuo, 1996). Finally, effective cation exchange capacity (ECEC) was determined through the summation method using acidity and exchangeable cations (Chapman, 1965).

2.6 Data modeling and Analysis

In the last decades, ordinary krigging (OK) interpolation remains one of the unbiased and superior linear spatial prediction methods for precision agriculture (Radocaj et al., 2021). In this study, we subjected the analyzed soil properties to the OK method in ArcGIS v.10 extensions geostatistical analyst tool to assess the accuracy of the interpolation and spatial autocorrelation. The present study employed dependent (SAVI and LST) and independent (soil nutrients) variables to assess the soil suitability for maize production (Fig 2). Furthermore, descriptive and geo-statistics methods were used to generate possible correlations. Thereafter, the soil properties were spatially interpolated using the Ordinary Krigging (OK) method in ArcGIS v.10.5 extension analyst geostatistical tool. Accuracy and cross-validation of soil properties were examined by semi-variogram modeling including the isotropic detection (equations 11 and 12) (Wang, 1999; Western et al. 2004).

$$Z* = (x_0) = \sum_{i=1}^{N} \lambda^1 z(x_i) \quad (11)$$

Where Z* represents the unknown sample at (x_0) location, while (x_1) represents known soil sampling values, is the sampled weighting coefficient and n is the neighborhood interpolated locations.

$$\gamma^{(h)} = \frac{1}{2N(h)} \sum_{i=1}^{n^{(h)}} [z(x_i)\text{-}z(x_i + h)]^2 \quad (12)$$

Where z (xi) is the value of the variable, is the lag, and N(h) is the pairs of sample points separated by h.

Accuracies of the interpolated soil properties, such as mean error (ME), root mean square error (RMSE), nugget (C_0), sill (C +C_0), and range (a) were used as indicators (Schloeder et al., 2001). The basic spatial parameter used in this study enables easy classification and characterization of soil properties. The formula described by Schloeder et al., (2001) in equations (13) and (14) was used to assess the ME and RMSE:

$$\text{ME} = \frac{1}{N} \sum_{i=1}^{N} [z(x_i)\text{-}\check{Z}(x_i)] \quad (13)$$

$$R\text{MSE} = \frac{1}{N} \sum_{i=1}^{N} [z(x_i)\text{-}\check{Z}(x_i)]^2 \quad (14)$$

2.7 Multi-criteria evaluation

The utilized AHP and weighted overlay method were used as dependent and independent variables for maize soil suitability. The independent and dependent variables were selected based on the proposed FAO land criteria evaluation and supported by Oluwatosin and Ogunkunle (1991), for rainfed maize soil suitability (Table 2). Thereafter, the AHT and weighted method were performed in ArcGIS 10 software. The criteria were further subjected to the Random inconsistency index (RI) and the consistency ratio was then calculated using the principal eigenvalue (Saaty, 2008). Afterward, the AHP and the comparison matrix were used to classify the soils into suitability classes using the formula described by Saaty, (1977) in equations (15) and (16).

$$\text{Weighted} = \sum_{i=1}^{N} Ci * W_n \quad (15)$$

Where Ci is the reclassified criterion and Wn is the weighted number of data.

$$S = f\,(x, \ldots\ldots, x_n) \quad (16)$$

Where S is the suitability level for land criteria.

Table 2. Modified maize soil suitability ratings for rainfed.

Suitability ratings (%) classes	100 Highly (S1)	85 Moderately (S2)	60 Marginally (S3)	< 40 Not suitable (N1)
RST variables				
Slope (%)	2-4	4-8	8-16	16-20
Rainfall at growing season (mm)	700-800	600-700	500-600	<500
PLST index (^{o}C)	22-25	20-22	18-20	16-18
drainage	Perfectly	Moderately	Imperfectly	poorly
PSAVI	0.37 – 0.79	0.22 – 0.37	0 – 0.218	-0.30 - 0
Soil variables (0-20cm)	I			
Total N (%)	0.08-0.15	0.08-0.04	0.02-0.04	<0.02
Avail P (mg/kg)	13-22	6-13	3-6	<3
Potassium (cmol kg $^{-1}$)	0.3-0.5	0.2-0.3	0.1-0.2	<0.1
Nutrient retention (n)				
ECEC (cmol kg $^{-1}$)	10-15	5-10	3-5	<3
Organic matter (g/kg)	3 - 4	2-3	1- 2	<1
Texture	Sandy clay loam	Sandy Loam,	Loamy sand	Sandy
(%)	15-40	40-60	60-75	75-90

S1: Highly (100%); S2: Moderately (85%); S3: Marginally (60%) and N1: Not suitable (<40%). Modified from Oluwatosin and Ogunkunle, (1991).

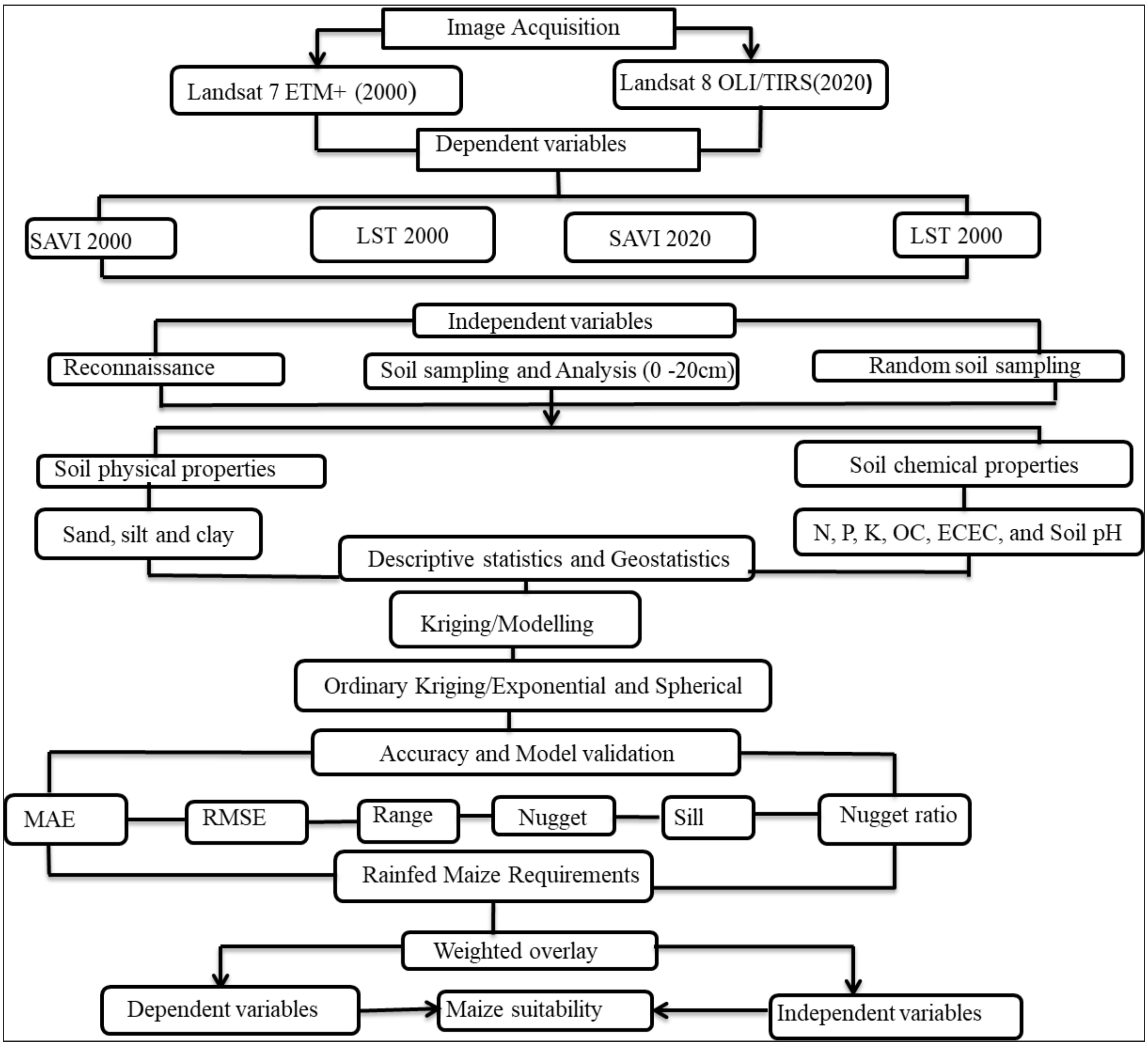

Figure 2. Workflow of the study.

3. Results and Discussion

3.1 Maize soils suitability using satellite-based covariates

Figures (3) and (4) showed that the SAVI and LST ranged from -1 (low) to 1 (high) in the study area. The observed low SAVI in the year 2020 suggests the presence of low vegetation cover and can therefore be traced to an increase in anthropogenic activities such as illegal tree felling and intensive cattle grazing. Moreover, deforestation and indiscriminate grazing are one of the threats faced by developing countries such as Nigeria (Nguetnkam and Dultz, 2011). Additionally, Staver et al., (2011) stated that pastoralism and deforestation tend to result in low soil nutrients, especially in the savanna region. Furthermore, Lie et al., (2013) pinpointed that SAVI techniques serve as one of the efficient spectral vegetation indices used for monitoring changes in soil properties, especially in an area with low vegetation cover. According to Frederiksen, (1993), SAVI is becoming an acceptable technique used in the support of crop nutrients assessment. The result of the present study can also be found in the study of Wu et al., (2018) who effectively correlate SAVI with soil pH and total nitrogen for a site-specific location using Landsat images.

The LST spatial variation of the study area ranged from 23.5^0 to $39.9\ ^0$ Celsius (See Fig 4). The sudden increase of the LST in the year 2020 could be a result of global climate change. It was also noticed that the study area is faced with consistent bush burning and deforestation. Moreover, according to Yao et al., (2004) sudden increase in surface temperature can lead to low crop yield. Besides, Wang et al. (2018) posit that a high increase in surface temperature can be regarded as a major environmental threat posed to crop farmers, especially in sub-Saharan Africa. The present study also coincides with the study carried out by Post et al., (1994) who utilized SAVI and LST as environmental covariates to study soil surface reflectance of soil properties for site-specific locations. Additionally, the spectral index random relationship observed in the present study is also by Sandholt et al., (2002).

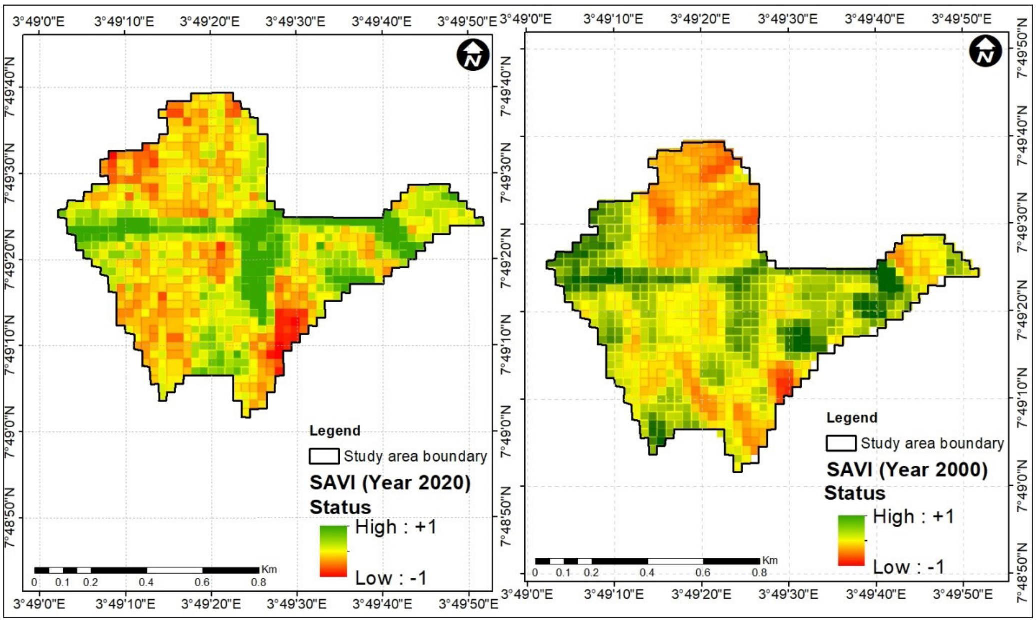

Figure 3. The predicted soil-adjusted vegetation index for the years 2020 and 2000.

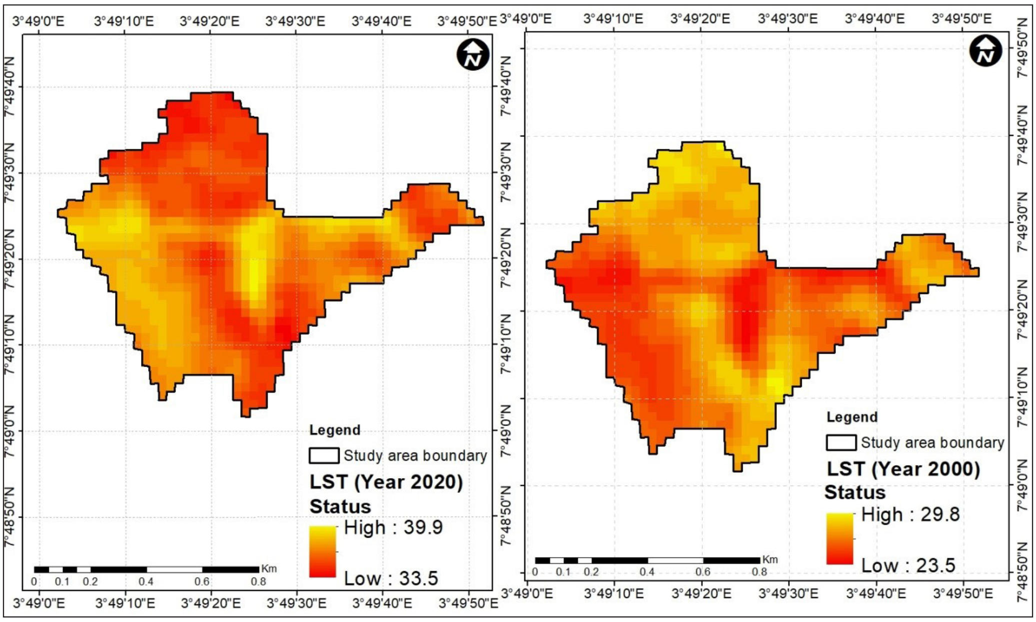

Figure 4. The predicted land surface temperature for the years 2020 and 2000.

3.2 Descriptive and correlation analysis of soil properties

Tables (3) and (4), show the description and correlation of the physical and chemical soil properties of the study area. The study reported by Carvalho et al., (2002) stated that when soil properties kurtosis and skewness values of soil properties are less than 3, such soil properties can be considered to have normal frequency distribution. From the results, it was observed that the majority of the soil properties had normal frequency distribution.

Table 3. Description of physical and chemical soil properties.

	Sand	Silt	Clay	OC	TN	Soil pH	ECEC	P	K
	(%)	(%)	(%)	(%)	(%)		mg kg^{-1}		cmol/kg
Min	85.8	3.0	4.1	1.2	1.1	3.0	3.8	2.0	1.2
Max	92.9	6.8	8.4	1.1	1.4	7.9	6.8	12.9	3.0
Median	88.4	5.4	5.7	1.0	1.3	3.9	7.1	5.8	1.2
Std. dev	3.0	1.6	1.8	1.1	1.8	2.0	1.0	4.9	1.5
Skewness	0.9	0.8	0.7	1.5	4.0	1.9	-2.0	0.4	2.0
Kurtosis	1.3	0.8	1.2	1.2	7.9	1.4	4.0	-0.4	3.2

Minimum (Min); Maximum (Max); Standard deviation (Std. dev)

Table 4. Soil correlation of the studied properties.

			OC	TN			Sand	Silt	Clay
	Soil pH	ECEC mg kg^{-1}	(%)		P mg kg^{-1}	K cmol/kg	(%)		
Soil pH	1								
ECEC	0.63	1							
OC	0.31	0.24	1						
TN	0.05	0.05	0.12	1					
P	0.15	-0.10	0.10	-0.17	1				
K	0.55	0.86	0.25	-0.10	-0.21	1			
Sand	0.02	0.03	0.00	0.01	0. 48	0.18	1		
Silt	0.09	0.02	0.01	0.06	0.29	0.89	-0.86	1	
Clay	0.08	0.00	0.01	0.04	0.30	0.88	-0.89	0.53	1

3.3 Spatial modeling of soil properties

In this study, the soil texture ranged from clay to sandy clay loam. Oluwatosin and Ogunkunle (2011) opined that soil texture within the range of sandy clay loam can be classified as suitable for maize production. The fertility soil distribution maps of the study area were produced using OK interpolated techniques. The soil TN ranged from (< 0.1%) very low to (0.2%) low. The low concentration of soil TN observed in the study area could be attributed to undulating topography or slope etc. Nevertheless, high P was observed with pockets of low concentration (Fig 5). The pH of the studied soils ranged from 5.6 (moderately acidic) and 7.3 (Neutral). The high soil OC distribution observed can be traced to litter or waste material decomposition in the study area (Fig 6). However, the inappropriate use of pesticides and fertilizers in the study area could be responsible for the soil to be acidic, and this interim with the result of Wang et al., (2018). In addition, the vicinities dumping of waste materials into seasonal rivers and streams which are sometimes used for irrigation could harbor toxic substances and therefore be responsible for the soils to moderately acidic. The spatial distribution concentration of K and ECEC concentration was also documented in the study soils (Fig 7).

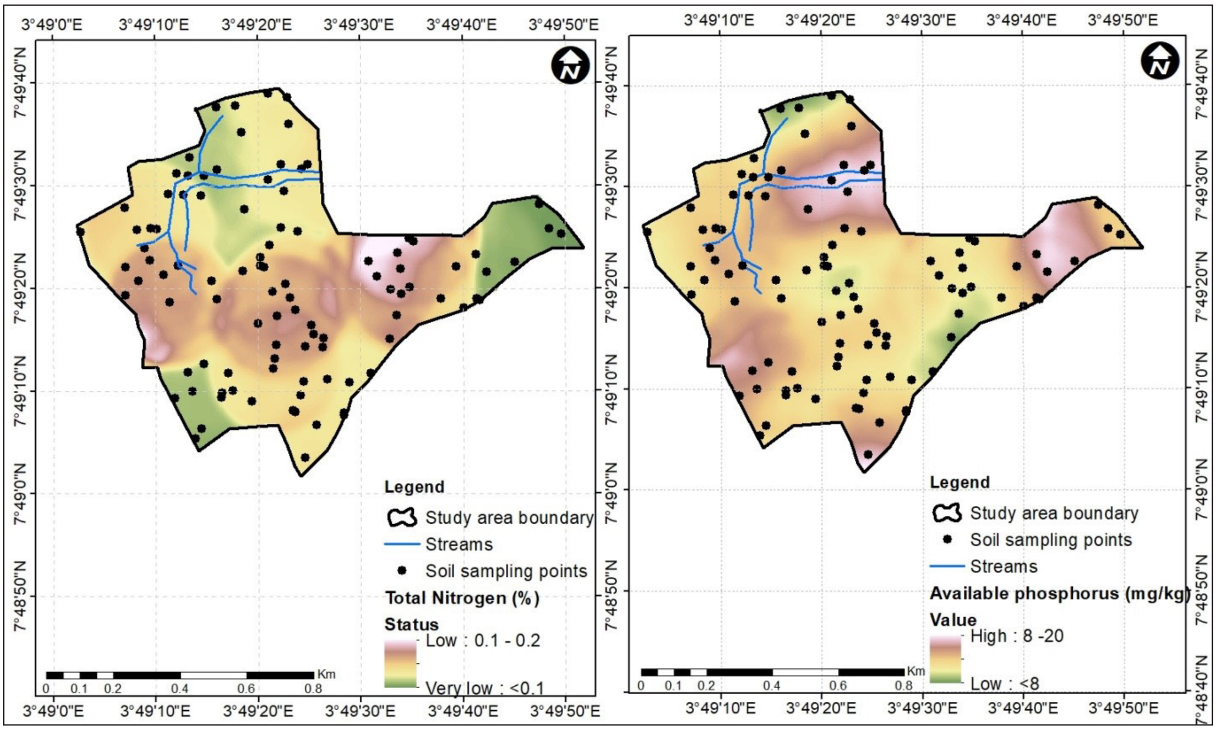

Figure 5. Distribution of total nitrogen and phosphorus.

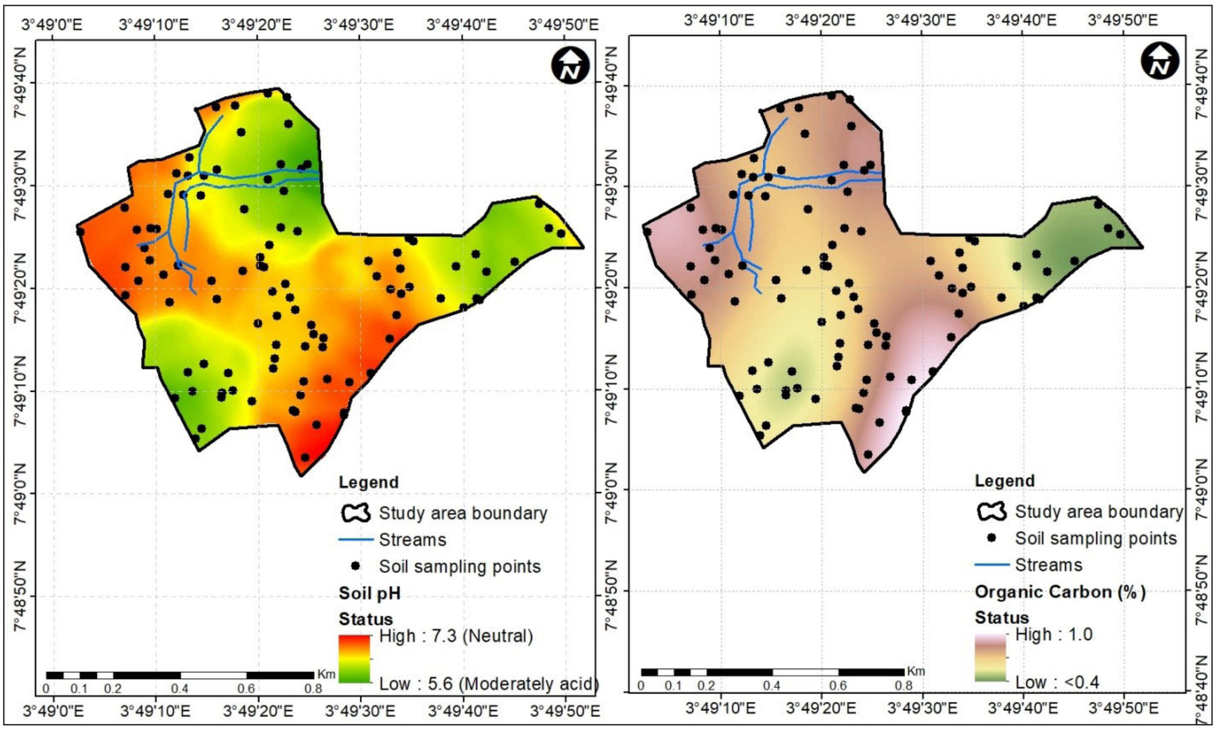

Figure 6. Distribution of soil pH and organic carbon.

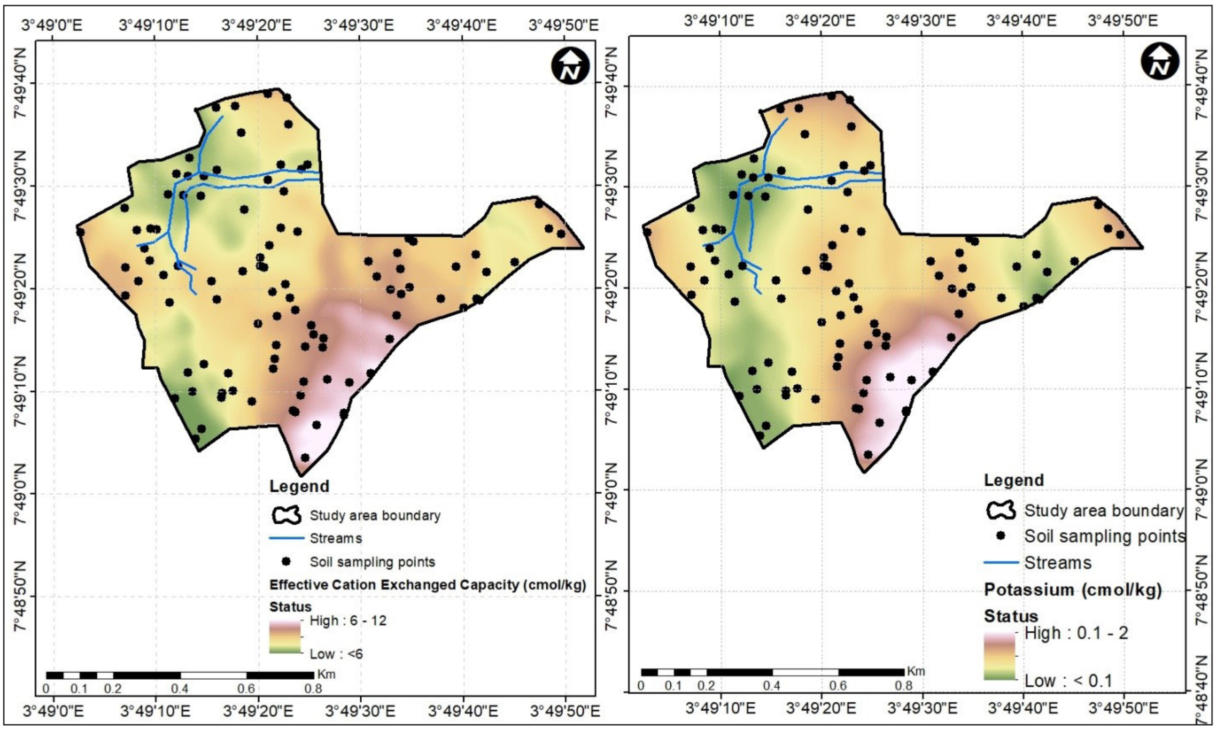

Figure 7. Distribution of effective cation exchanged capacity and potassium.

The ME and RMSE were used to identify the accuracy of the soil properties using OK interpolation (Table 5). The ME and RMSE values showed that the interpolated soil properties had lower nugget effects when a model with exponential. According to Robertson, (2008), soil properties with low nuggets have been widely used for site-specific agriculture. In the present study, a ratio less than 25% (percent) means strong spatial variance and those within the ratio of 25 % and 75 % means moderate distribution of soil properties, therefore, from the interpolated soil analysis, soil pH, K, OC, and silt soil texture gave the strong spatial dependency for an exponential model, while the spherical model provided moderate spatial dependency for TN, P, CEC, clay, and sand. However, the moderate spatial dependency can be traced to an increase in human activities such as erosion hazards, abuse of fertilizer, and global climate change (Cambardella et al. 1994). The results of the present study are also following the research conducted by Venteris et al., (2014).

Table 5. Accuracy and validation of soil properties.

	Model	ME	RMSE	Range (m)	Nugget (C0)	C0/(CO+C)	Nugget ratio (%)
Soil pH	EX	0.3	0.9	264	0.05	0.21	21
N (%)	SP	0.1	0.8	236	12.9	0.30	30
K (cmol/kg),	EX	0.2	0.5	269	16.1	0.16	16
P (mg kg^{-1})	SP	0.4	3.3	214	11.66	0.44	44
OC (%)	EX	0.4	0.1	267	0.03	0.13	13
CEC (cmol/kg)	SP	0.2	1.2	271	0.01	0.50	50
Sand (%)	SP	0.3	11	972	0.06	0.58	60
Silt (%)	EX	0.1	0.6	254	0.04	0.24	24
Clay (%)	SP	0.4	3.9	567	0.09	0.60	60

EX: Exponential, SP: Spherical

3.4 Maize soil suitability using AHP and weighted overlay

The dependent and independent layers based on the AHT and weighted techniques were used to assess the maize suitability using a pairwise comparison matrix (Table 6). The present study employed a scale of 0 to 100 % to itemize the procedure and a 7.5 % ratio was obtained for consistency. The soil fertility distribution and thematic map layers of the PLST, PSAVI, existing river, and soil map of the study area were coupled together and produced in a raster format. The results of the thematic layers were rated in the following order: 35 % (soil nutrients), 20 % (LST), 20 % (SAVI), 15 % (river), and 10 % (road) to produce the maize soil suitability of the area (Fig 8).

Table 6. Weights criteria using pairwise comparison.

	Soil nutrients	PLST	PSAVI	River	Road	Priority	Scale
Soil nutrients	2	1	1	0.5	1	35	1
PLST	1	0.5	2	1	0.5	20	2
PSAVI	0.5	1	0.5	1	1	20	3
River	0.5	1	1	0.5	0.5	15	4
Road	1	0.5	1	1	0.5	10	5

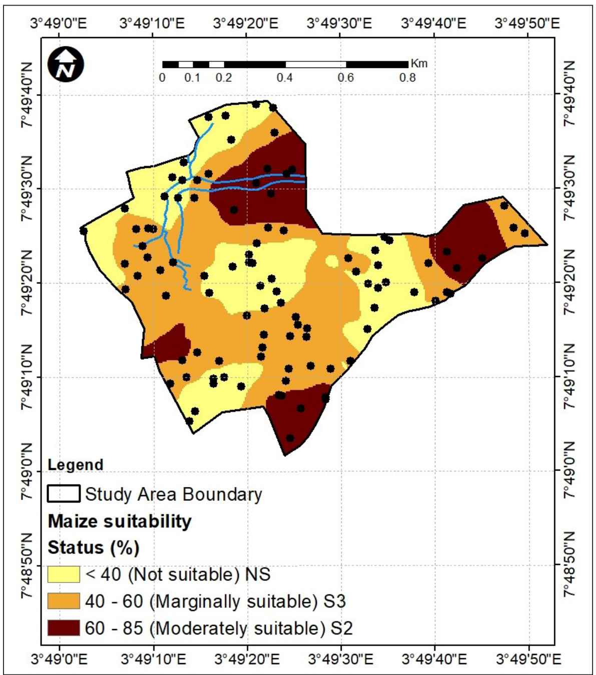

Figure 8. Maize soil suitability.

4. Conclusions

The study focused on the variability assessment of soil nutrients and its impacts on soil suitability for maize production using remote sensing (RS) and geographic information system (GIS) techniques. The increase and awareness of precision agriculture have necessitated the integration of GIS, RS, and geo-statistics methods, especially in the spatial environment of today. The combined GIS and RS techniques through multi-criteria have assisted in efficiently mapping the soil nutrients of the area in less time and with higher accuracy for maize production. The AHT shows that RS variables - LST, SAVI, and the interpolated soil properties can help individual or soil users, especially farmers to identify suitable land areas for precision farming and optimum crop production. The soil fertility distribution maps generated showed that the exponential model gave the lowest values of ME and RMSE than the spherical model. However, the weighted overlay and AHT used helped to partition the studied soils into moderately (85%), marginally (60%), and not suitable (40%) for maize production. The limiting factors were an increase in anthropogenic activities (such as abuse of pesticides or fertilizers), an undulating slope, an increase in surface temperature, and erosion hazard. The present study proved that integration of OK, AHT coupled with remotely sensed-based spectral indices such as LST and SAVI will help farmers and policy-makers for sustainable and precision agriculture.

5. Data availability statement

The data that support the findings of this study are not available but can be provided upon reasonable request.

Acknowledgment

The author wishes to thank the authorities of the Institute of Agricultural Research and Training Moor Plantation, Ibadan, Obafemi Awolowo University for their support and understanding.

References

Adekiya, A.O., Agbede T.M., (2009). Growth and yields of tomato (Lycopersicon esculentum Mill) as influenced by poultry manure and NPK fertilizer. Emirate Journal of Food Agriculture; 21(1): 10–20.

Bouyoucos, G.H., (1962). Hydrometer method for making particle size analysis of soils. Agronomy Journal 54: 464-465. DOI: 10.2134 /agronj1962.00021962005400050028x.

??Bremner, J. M., & Mulvaney, C. S. (1982). Nitrogen-Total.

Cambardella. C.A., Moorman. T.B.,Novak, J.M., Parkin, T.B., Karlen, D.L., Turco. R.F, and Konopka, A.E, (1994). Field–scale variability soil properties in central Iowa soils. Soil Science Society of American Journal 58:1501-1511. doi:10.2136/sssaj1 994.03615995005800050033x.

Chinese Journal of Applied Ecology. 2018; 29. https://doi.org/10.13287/j.1001-9332.201803.038

Carvalho, J. d., Silveira, P. d., & Vieira, S. R. 2002. Geoestatística na determinação da variabilidade espacial de características químicas do solo sob diferentes preparos. Pesquisa Agropecuária Brasileira, 37(8), 1151-1159.

Dorigo, W., Richter, R., Muller, A., (2005). A lookup table approach for biophysical parameter retrieval by radioactive transfer model inversion is applied to the wide field of view data. In: Proceedings of the Fourth EARSeL Workshop on Imaging Spectroscopy, Warsaw, Poland.

Ekeleme, F., Jibrin, J.M., Kamara, A.Y., Oluoch, M., Samndi, A.M., Fagge, A.A. Assessment of the relationship between soil properties, Striga hermonthica infestation and the on-farm yields of maize in the dry Savannas of Nigeria. Crop Prot. (2014) 66, 90–9

FAO. Guidelines for soil description. Rome: FAO; (2007). Page. 109.

FDALR. The Reconnaissance Soil Survey of Nigeria. 1990; volume. 2.

Frederiksen, P. (1993). Satellite-based assessment and monitoring of land degradation in semi-arid tropical Africa: aspects of the soil/vegetation complex.

Ge, F.L., Zhang, J.H., Su Z.G., Nie X.J., (2007) Response of changes in soil nutrients to soil erosion on a purple soil of cultivated sloping land. Acta Ecol Sin 27:459–463. doi: 10.1016/s1872-2032(07)60018-3

Jeevalakshmi, & Manikiam, B. (2017). Land Surface Temperature Retrieval from LANDSAT data using Emissivity Estimation.

Jesus, J. B., Santana, I. D. M., (2017). Estimation of land surface temperature in caatinga area using Landsat 8 data, 7, 150157. Retrieved from https//periodicos.ufpe.br/revistos/hrs/article/view/22766101 (3) , 366-378

Jiang, Z., Huete, A. R., Chen, J., Chen, Y., Li, J., Yan, G., 2006. Analysis of NDVI and scaled difference vegetation index retrievals of vegetation fraction. Remote Sensing of Environment,

Liu L, Wang H., Dai W, Lei X., Yang X, Li X (2015) Spatial variability of soil organic carbon in the forestlands of northeast China. J For Res 25 (4): 867–876.

Marko K., Elfeki A.M.M., Alamri N.S (2014). Geostatistical analysis using GIS for mapping groundwater quality: a case study in the recharge area of Wadi Usfan, western Saudi Arabia. Arab J Geosci 7:5239–5252

Martey, E., Wiredu, A. N., Etwire, P. M., Fosu, M., Buah, S. S. J., Bidzakin, J., Kusi, F. (2014). Fertilizer adoption and use intensity among smallholder farmers in Northern Ghana: A case study of the AGRA soil health project. Sustainable Agriculture Research, 3, 24–36. doi:0.5539/sar.v3n1p24.

McLean E.O. pH and lime requirements. In: Page ALE, editor. Methods of Soil Analysis. Madison, WI, USA: American Society of Agronomists Inc.; (1982)

Nelson, D.W., Sommers, L.E., (1996). Total carbon, organic carbon, and organic matter. In: Sparks et al. (Eds.), Methods of Soil Analysis. Part 3: Chemical methods. SSSA, Madison, WI, USA.

Oluwatosin, G. A., Ogunkunle, A. O., (1991). Suitability rating of some soils of the savanna zone of South-western Nigeria for rainfed Maize. Nigeria Journal of Soil Science 10: 1-24.

Nguetnkam, J.P., & Dultz, S. (2014). Clay dispersion in typical soils of north Cameroon as a function of ph and electrolyte concentration. Land Degradation & Development, 25.

Rasul, A., H., Balzter, C., Smith, 2015. Spatial Variation of the Daytime Surface Urban Cool The island during the Dry Season in Erbil, Iraqi Kurdistan, from Landsat 8." Urban Climate 14: 176–186.doi:10.1016/j.uclim.2015.09.001.

?Relationship between soil color and Landsat reflectance on semiarid rangelands. Soil Science Society of America Journal 58: 1809 ± 1826.

Radocaj, D., Juriši´c, M., and Antoni´c, O., (2021). Determination of Soil C:N Suitability Zones for Organic Farming Using an Unsupervised Classification in Eastern Croatia. Ecol. Indic. 123, 107382.

Robertson, G.P., (2008). In: GS+: Geostatistics for the Environmental Sciences. Gamma Design Software. Plainwell, Michigan, USA.

Saaty, T.L., (1977). The Analytic Hierarchy Process: Planning, Priority Setting. Resource Allocation. McGraw-Hill International, New York, NY, USA.

Saaty, T.L., (2008). Decision-making with the analytic hierarchy process. Int. J. Services Sciences, Vol. 1, pg 83–98.

Sandholt I., Rasmussen K., Andersen J (2002). A simple interpretation of the surface temperature/vegetation index space for assessment of surface moisture status. Remote Sens Environ 79:213–224.

Sys, I., E. Van-Ranst, and J. Debveye. (1991). Land evaluation. Part 1: principles in land evaluation and crop production calculations. General Administration for Development Cooperation, Brussels, Belgium (Agricultural Publications No. 7).

Staver, A. C., S. Archibald, and S. A. Levin. (2011). The global extent and determinants of savanna and forest as alternative biome states. Science 334:230–232.

Schloeder C.A., Zimmermen NE., Jacobs M.J (2001). Comparison of methods for interpolating soil properties using limited data. Soil Sci Soc Am J 65:470–479.

USDA Soil Taxonomy. Soil Survey Staff, Agriculture Handbook, No. 436, 2nd ed. Washington, DC: United States Department of Agriculture, Natural Resources Conservation Service; (1999). p. 869.

United Nations. (2017). World Urbanization Prospects: The Revision United Nations (Population Framework for decision support tools for integrated soil fertility management in sub-Saharan Africa (Draft). Paper presented at the African Soil Health Consortium inaugral workshop.

Venteris, E., Basta, N., Bigham, J., Rea, R., (2014). Modeling spatial patterns in soil arsenic to estimate natural baseline concentrations. J. Environ. Qual. 43 (3), 936–946.

Wu, B., Guo, S.H., Li, B.L., Zhang LY. Draft of soil environmental function regionalization of China.

Walkley, A., Black, I. A., (1939). An examination of Degtjareff method for determining soil 714 organic matter and a proposed modification of the chronic acid titration method.Soil Science, 71537, 29 – 38. DOI: 10.1097/00010694193401000-00003.

Wang, X., Ma, X., & Yan, Y. (2017). Effects of soil C: N:P stoichiometry on biomass allocation in the alpine and arid steppe systems. Ecology and Evolution, 7, 1354 - 1362.

Western, A. W., S.-L. Zhou, R. B. Grayson, T. A. McMahon, G. Blöschl and D. J. Wilson (2004) Spatial correlation of soil moisture in small catchments and its relationship to dominant spatial hydrological processes. Journal of Hydrology, 286 (1-4), pp. 113-134.

Warrick, A.W., (1998) Spatial variability. In Environmental soil physics, ed. D. Hillel, 655–675. San Diego, Calif.: Academic Press.

Wang, Z. Q., (1999), Geostatistics Applied in Ecology. Beijing: Science Press. 109-126 [in Chinese]

Yao, X., Fu, B., Lu, Y., Sun, F., Wang, S., Liu, M., (2004). Comparison of four spatial interpolation methods for estimating soil moisture in a complex terrain catchment. PLoS ONE 8 (1)

Zhang, Z., Yu, D., Shi, X., Weindorf, D.C., Sun, Y., Wang, H., Zhao, Y. (2010). Effects of prediction methods for detecting the temporal evolution of soil organic carbon in the Hilly Red Soil Region, China. Environ. Earth Sci., 64, 319–328.